Total Charge Movement per Channel

The Relation between Gating Charge Displacement and the Voltage Sensitivity of Activation

Daniel Sigg and Francisco Bezanilla

From the Department of Physiology and Department of Anesthesiology, School of Medicine, University of California, Los Angeles, Los Angeles, California 90095

ABSTRACT One measure of the voltage dependence of ion channel conductance is the amount of gating charge that moves during activation and vice versa. The limiting slope method, introduced by Almers (Almers, W. 1978. *Rev. Physiol. Biochem. Pharmacol.* 82:96–190), exploits the relationship of charge movement and voltage sensitivity, yielding a lower limit to the range of single channel gating charge displacement. In practice, the technique is plagued by low experimental resolution due to the requirement that the logarithmic voltage sensitivity of activation be measured at very low probabilities of opening. In addition, the linear sequential models to which the original theory was restricted needed to be expanded to accommodate the complexity of mechanisms available for the activation of channels. In this communication, we refine the theory by developing a relationship between the mean activation charge displacement (a measure of the voltage sensitivity of activation) and the gating charge displacement (the integral of gating current). We demonstrate that recording the equilibrium gating charge displacement as an adjunct to the limiting slope technique greatly improves accuracy under conditions where the plots of mean activation charge displacement and gross gating charge displacement versus voltage can be superimposed. We explore this relationship for a wide variety of channel models, which include those having a continuous density of states, nonsequential activation pathways, and subconductance states. We introduce new criteria for the appropriate use of the limiting slope procedure and provide a practical example of the theory applied to low resolution simulation data.

KEY WORDS: limiting slope • thermodynamics • Monte Carlo • gating current • voltage dependence

INTRODUCTION

The sine qua non of voltage-dependent ion channels is their ability to alter ion permeability of membranes in response to changes in the transmembrane potential. Hodgkin and Huxley (1952) accounted for the voltage sensitivity of Na^+ and K^+ conductance in the squid giant axon by postulating charge movement between kinetically distinct states of hypothetical "activating particles". With the advances that have been made in the biochemistry and molecular biology of ion channels since then, we now recognize that the embodiment of their "activating particle" resides in the ion channel itself, as a structural component, though the molecular details of the voltage sensitive "gating" of the pore remains largely unknown. The first verification of gating charge movement was by Armstrong and Bezanilla (1973), who recorded nonlinear capacitive current transients from tetrodotoxin (TTX) blocked Na channels in the squid axon. An important quantity that characterizes the voltage sensitivity of the channel is the range of gating charge displacement Δq energetically linked to channel activation. The most significant advancement in measuring Δq that followed the work of Hodgkin and Huxley was due to Almers (1978), who treated the case of a linear sequence of discrete closed states followed by a single open state (Almers' criterion, see Fig. 1 *A*). Almers stated that for such a model, the following relation holds:

$$\lim_{V \to -\infty} kT \frac{\mathrm{d} \ln(P_o)}{\mathrm{d}V} = \Delta q\,, \qquad (1)$$

where P_o is the fraction of time the channel is open at equilibrium (open probability), V is the membrane potential in millivolts, and kT is the characteristic thermal energy (Boltzmann constant times absolute temperature $\simeq$ 25 milli-electron volts at room temperature). The experimental use of Eq. 1, often referred to as the limiting slope procedure, has been used by many investigators to estimate total gating charge movement of activation (e.g., Stimers et al., 1985; Liman et al., 1991; Papazian et al., 1991; Schoppa et al., 1992; Zagotta et al., 1994).

The Q/N technique is an alternative to the limiting slope method and is a direct determination of gating charge movement per channel. Independent measurements of the total charge Q and the number of channels N are made in a single preparation, and the ratio,

Address correspondence to Dr. F. Bezanilla or D. Sigg, Department of Physiology, UCLA School of Medicine, Los Angeles, CA 90095. FAX: 310-794-9612; E-mail: pancho@cvmail.anes.ucla.edu

$\Delta q_{Q/N}$, is then calculated. The first reliable value of $\Delta q_{Q/N}$ was published by Schoppa et al. (1992), who recorded from a single patch containing *Shaker* K^+ channels expressed in *Xenopus* oocytes. They obtained a $\Delta q_{Q/N}$ of 12.3 eu (electronic unit of charge $\simeq 1.602 \times 10^{-19}$ Coulombs)[1] per channel, which has since been verified by our lab and others (Aggarwal and MacKinnon, 1996; Noceti et al., 1996; Seoh et al., 1996). A similar value was obtained from a mutant channel in which the hydrophobic residue Leu^{370}, located in the putative voltage sensing domain of *Shaker* (the S4 transmembrane segment), was replaced with valine. Their finding of no change in $\Delta q_{Q/N}$ in the mutant compared to the unmutated channel was expected since the net charge of the protein was unchanged. However, use of the limiting slope procedure on the two channels yielded values that were significantly lower than $\Delta q_{Q/N}$: 9.5 eu for the unmutated channel and 5.5 eu for the mutant (Schoppa et al., 1992). The discrepancy between the results from the Q/N technique and the limiting slope procedure might be explained by the existence of gating charge movement which is dissociated from the activation process, making no contribution to voltage sensitivity of opening. This noncontributing charge component may take on two forms: gating charge movement occurring after the channel has opened (latent charge movement) and charge movement that is independent of the activation process (peripheral charge movement). The limiting slope procedure, in contrast to the Q/N technique, measures only the range of charge movement which is energetically linked to channel opening (activation charge movement), ignoring the latent and peripheral charge movements. In their conclusion, Schoppa et al. were careful to point out that, despite the possibility that latent and/or peripheral charge movement exists in *Shaker,* the most likely source for the reduced limiting slope values was lack of experimental resolution. Indeed, there has been sharp criticism of the reliability of the limiting slope procedure from various authors (Anderson and Koeppe, 1992; Bezanilla and Stefani, 1994; Zagotta et al., 1994). The chief reasons for the skepticism in the validity of the technique are: (*a*) the inability to accurately determine where the limiting value of the slope occurs on the voltage axis and (*b*) the difficulty of measuring the low values P_o required to reach that value (typically $<10^{-3}$).

In this paper, we address the problem of poor resolution in the limiting slope procedure by introducing a measure of the progress of activation named the activation charge displacement, q_a. Plotting mean activation charge displacement $\langle q_a \rangle$ versus voltage is a more reliable way of estimating limiting slope, and, furthermore, there is a relation between $\langle q_a \rangle$ and mean gating charge displacement, $\langle q \rangle$, which makes the additional measurement of gating currents a valuable tool in interpreting limiting slope data (for example, the gating current recordings by Schoppa et al. (1992) can be used to predict the amount by which they underestimated Δq with the limiting slope technique). We develop the theory to include models containing an arbitrary number and arrangement of states (including continuum models) and allow for multiple open states with different conductances. We follow with a series of examples illustrating the theory, ending with a sample analysis of low resolution simulated data. We conclude with a summary of results and an approach for applying the limiting slope method in practice.

Theory

Nature of the model. We preface the discussion of specific models by stating assumptions regarding their general nature. We assume that after a sudden step in membrane potential, the occupancy distribution of the channel propagates through a network of conformational states representing the activation pathway. The reaction coordinate is the gating charge displacement (q). To place the quantity q in its proper context, we note that the mean gating current for N channels $\langle I_g \rangle$ is $N\mathrm{d}\langle q \rangle/\mathrm{d}t$ and the plot of $N\langle q \rangle$ vs. voltage is the Q-V curve. There may be more than one state for a given value of q, which allows for loops and parallel pathways in the activation sequence (see Fig. 1 *B*). Since the mean $\langle q \rangle$ is an extensive state variable, q has a specific value for every state in the model. In addition, states are assigned a potential of mean force $F(q,\xi,V)$ and a fractional conductance $f(q,\xi)$. Both are assumed to be defined by the value of q and other degrees of freedom indicated by ξ, and, in the case of F, also the membrane potential V. In terms of the variable ξ, we will be primarily concerned with degrees of freedom produced by states that are degenerate with respect to q. An example is a branching of the activation path, producing a duplication of states. Accordingly, in some cases it is useful to include a degeneracy factor ϕ, which for a nondegenerate state has the value of one. We assume for the purpose of derivations that all gating charge is energetically coupled to the activation process (essential charge), since only essential charge contributes to the voltage sensitivity of activation. We shall consider the effect of peripheral charge in Fig. 4. The fractional conductance is defined as the ratio of the state conductance $g(q)$ to the maximal value at the given potential, g_o. We assume a linear voltage-dependence of $F(q,V)$ (e.g., Tsien and Noble, 1969):

$$F(q,V) = G(q) - qV, \qquad (2)$$

[1] *Abbreviation used in this paper:* eu, electronic unit of charge $\simeq 1.602 \times 10^{-19}$ Coulombs.

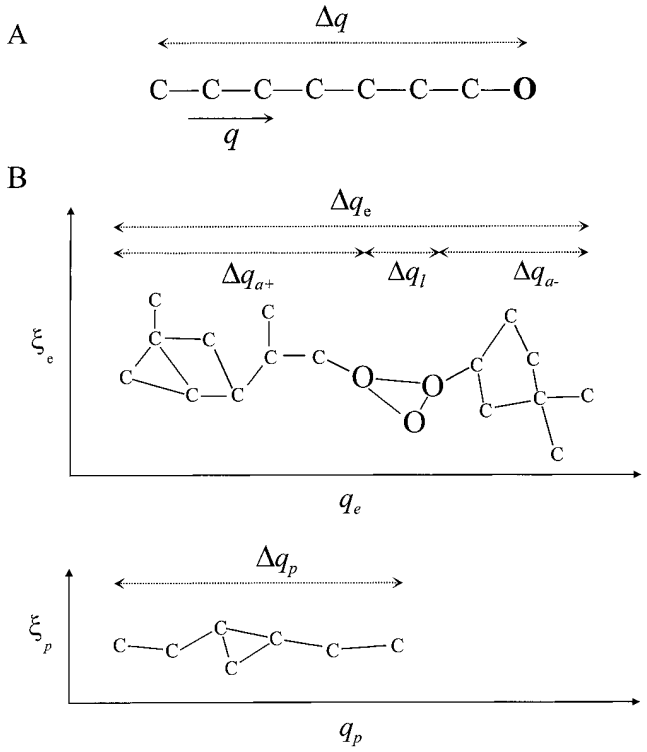

FIGURE 1. (*A*) An example of a kinetic model satisfying Almers' criterion for Eq. 1. It consists of a linear sequence of discrete closed states followed by a single open state. The total range in gating charge displacement is Δq. A more generalized model (*B*) includes degeneracies produced by additional degrees of freedom (indicated by the variable ξ), multiple open states, and peripheral charge movement. In a discrete model with no subconductance states we can graphically display the range in essential charge movement, Δq_e, as a sum of its components; Δq_{a+} and Δq_{a-} are the range in positive and negative activation charge displacement, respectively, and Δq_l is the range in latent charge displacement. The peripheral charge movement, Δq_p, is shown on the lower panel with its own reaction coordinate, indicating independence from the main activation sequence. The total charge movement per channel is $\Delta q = \Delta q_e + \Delta q_p$, which is the value obtained from the Q/N procedure ($\Delta q_{Q/N}$). Use of the limiting slope procedure estimates the value of Δq_{a+} in the hyperpolarizing direction and Δq_{a-} in the depolarizing direction. In a saturated channel, Δq_l and Δq_p are zero.

where $G(q) = F(q,0)$ and depends on thermodynamic variables other than voltage such as temperature and pressure. By assigning a set of variables to each state rather than a difference of values between states (as is often done in describing kinetic models), we assure that the model automatically obeys detailed balance and conservation of charge density around any loops in the kinetic model. In this paper we consider only thermodynamic quantities, so we ignore the nature of pathways between states that determine kinetics. We require only that equilibration occurs between states on a time scale which is faster than that of our method of measurement (see Fig. 9 and corresponding text).

Definition of terms. The word activation refers to the process of opening the channel pore. Technically, then, a blocked channel does not activate, but in such cases we alter the definition to include any conformational changes in the channel protein that produces a change in gating charge displacement. Without loss in generality, we assume that conducting channels activate with increasing membrane potential, since most classes of ion channels conform to this behavior. However, the theory outlined below is easily applied to a channel that opens with hyperpolarization by making trivial changes in sign. We formally define gating charge displacement q as any nonlinear capacitive charge movement in a single channel, regardless of whether it makes an energetic contribution to opening (activation coupling) or not. The variable q serves as a convenient reaction coordinate of activation. The value of q in the limit $V \to -\infty$ is referenced to zero. The maximum value of q at depolarizing potentials is by definition the total gating charge movement per channel Δq, which is measurable experimentally with the Q/N procedure, i.e. $\Delta q = \Delta q_{Q/N}$. The component of q which is activation coupled is the essential charge displacement (q_e) and the remainder is the peripheral charge displacement (q_p). The latter does not contribute to the voltage sensitivity of the channel. The open probability (P_o) is defined for a population of channels as the ratio of the mean conductance to the maximum conductance. We introduce the activation potential ($W_a = -kT\ln[P_o]$), which is a measure of the electrical energy needed to open the channel. Finally, we define the activation charge displacement (q_a) through its mean value, which equals the negative gradient of the activation potential: $\langle q_a \rangle = -\mathrm{d}W_a/\mathrm{d}V$. Note that if P_o is multiplied by a constant it does not affect the value of $\langle q_a \rangle$, i.e.,

$$\langle q_a \rangle = kT\frac{\mathrm{d}\ln(cP_O)}{\mathrm{d}V} = kT\frac{\mathrm{d}\ln P_O}{\mathrm{d}V}. \qquad (3)$$

This is useful experimentally since the value of P_o obtained from analysis of macroscopic ionic current traces is usually defined only within a multiplicative constant. In the next two sections we will derive a relationship between the mean activation charge and gating charge displacements that will serve as the foundation for developing a practical approach in measuring essential gating charge movement.

Finite number of states. We start with models that contain a finite number of discrete states, by which we mean that the time spent by the channel during the transition from one state to another is negligible compared to the dwell times in the states themselves. For the purpose of this derivation, and the one following which deals with continuum models, all gating charge movement is essential (i.e., $q = q_e$). Each state i is completely specified by the state variables (q_i, G_i, f_i) as well

as an optional degeneracy factor ϕ_i. Subconductance states are produced when $0 < f_i < 1$. The open probability of a single channel at equilibrium is $P_o = \langle g \rangle / g_o$, where g_o is the open pore conductance, and $\langle g \rangle$ is the average conductance.

$$\langle g \rangle = \sum_i g_i p_i = g_O \sum_i f_i p_i . \quad (4)$$

The p_i are the equilibrium state probabilities which are found using the normalized Boltzmann distribution:

$$p_i = \frac{\phi_i \exp \frac{-F_i}{kT}}{\sum_i \phi_i \exp \frac{-F_i}{kT}} . \quad (5)$$

The denominator in Eq. 5 has the form of a coarse-grained partition function. From Eqs. 4 and 5 we obtain an expression for the mean open probability:

$$P_O = \frac{\sum_i f_i \phi_i \exp \frac{-F_i}{kT}}{\sum_i \phi_i \exp \frac{-F_i}{kT}} . \quad (6)$$

Then, using the linear relation of Eq. 2, which for a discrete model has the form:

$$F_i = G_i - qV , \quad (7)$$

we evaluate the derivative of $\ln(P_o)$ using Eqs. 6 and 7:

$$\langle q_a \rangle \equiv kT \frac{d \ln P_O}{dV} = \frac{\sum_i q_i f_i \phi_i \exp \frac{-F_i}{kT}}{\sum_i f_i \phi_i \exp \frac{-F_i}{kT}} - \frac{\sum_i q_i \phi_i \exp \frac{-F_i}{kT}}{\sum_i \phi_i \exp \frac{-F_i}{kT}} . \quad (8)$$

The two terms on the right side of Eq. 8 are averages over q. The first term uses a reduced partition function where each term is weighted by the fractional conductance of the corresponding state. The second term, which sums over all states, is the average gating charge displacement $\langle q \rangle$, which, in the absence of peripheral charge movement, is proportional to the experimentally derived Q-V curve. We rewrite Eq. 8 as:

$$\langle q_a \rangle = \Delta q - \frac{\sum_i (\Delta q - q_i) f_i \phi_i \exp \frac{-F_i}{kT}}{\sum_i f_i \phi_i \exp \frac{-F_i}{kT}} - \langle q \rangle . \quad (9)$$

The second term on the right of Eq. 9, which sums over states that have at least partial conductance, represents the mean latent charge displacement ($\langle q_l \rangle$). In the expression for $\langle q_l \rangle$, the quantity that is being averaged over is $\Delta q - q$, which has its origin where the gating charge displacement reaches its largest value (i.e., $q = \Delta q$) and increases with decreasing value of q. Thus, for example, the open state in the model of Fig. 1 *A*, although it conducts ($f \neq 0$), contributes nothing towards the value of $\langle q_l \rangle$ because it lies to the right of all the other states, at the value of maximum gating charge displacement.

Finally, after moving $\langle q_l \rangle$ to the left side of the equation, we have:

$$\langle q_a \rangle + \langle q_l \rangle = \Delta q - \langle q \rangle . \quad (10)$$

The relationship between the activation and essential charge displacements is now clear. The sum of the activation and latent charge displacement curves ($\langle q_a \rangle + \langle q_l \rangle$) superimposes onto that of the mean gating charge displacement $\langle q \rangle$ by simply inverting and shifting upwards by Δq. In the event that $\langle q_l \rangle$ vanishes or remains constant for all potentials, $\langle q_a \rangle$ can be superimposed onto $\langle q \rangle$. In such cases, we say that the channel is saturated with activation charge, since the total range of activation charge displacement (Δq_a) matches the charge movement per channel, Δq. In a saturated channel, knowledge of the shape of $\langle q \rangle$ versus voltage, obtainable from a Q-V measurement, allows one to predict the range in potentials where $\langle q_a \rangle$ reaches its limiting value. A model that satisfies Almers' criterion (Fig. 1 *A*) is obviously saturated. However, so are kinetic models with a more complicated arrangement (loops and parallel pathways) of closed states that converge onto a single or degenerate set of open state(s). The requirement for saturation is twofold: (*a*) the activation sequence has only one open state, or, if there is a cluster of open states, they must all have the same value of q; (*b*) there is no peripheral charge movement. If the first requirement is satisfied, but not the second, then we can speak of saturation of the essential activation sequence. However, the presence of peripheral charge movement may contaminate the shape of the Q-V, making it less useful for limiting slope analysis. In any case, Eq. (10) can be made generally valid even when there is peripheral charge movement by replacing q with q_e.

Continuous density of states. A similar analysis can be applied to a continuous system. Here, the partition function becomes an integral over a continuum of states. We maintain the condition that the only variable to be summed over is the gating charge q. The meaning of $f(q)$ in a continuum model may be best thought of as a conditional probability relating q to the likelihood that the pore is open. With these considerations in mind, the derivation follows exactly that of the discrete state model. The continuum analogue of Eq. 6 is:

$$P_O = \int f(q)\, p(q)\, dq = \frac{\int f(q)\, \phi(q) \exp \frac{-F(q,V)}{kT} dq}{\int \phi(q) \exp \frac{-F(q,V)}{kT} dq} \quad (11)$$

From Eq. 11, we immediately obtain the counterpart to Eq. 9:

$$\langle q_a \rangle = \Delta q - \frac{\int (\Delta q - q)\, f(q)\, \phi(q) \exp\frac{-F(q,V)}{kT} dq}{\int f(q)\, \phi(q) \exp\frac{-F(q,V)}{kT} dq} - \langle q \rangle . \quad (12)$$

As we did in the case of discrete models, we identify the second term on the right of Eq. 12 as the latent charge position $\langle q_l \rangle$. Obviously, $\langle q_l \rangle$ cannot be made to vanish or even maintain a constant value with respect to voltage without rendering the channel permanently closed. This is because, in order for the channel to conduct at all, $f(q)$ must have a nonvanishing value across some range of the continuous variable q. In other words, it is meaningless to speak of a single open state in a continuum model, and so the channel will never be saturated with activation charge. However, one can come close (within experimental resolution) by allowing the channel to be open only for a range of values of q near its maximum value (e.g., see Fig. 7).

METHODS

Numerical Computation of Activation Curves

Activation curves of discrete state models were calculated using Eqs. 5 to 7, 9, and 10 from the array of state variables (q_i, G_i, f_i) and degeneracy factors ϕ_i that define a particular model. Continuum models were evaluated using the same algorithm by increasing the number of "states" to 2,000. It was found that as few as 50 states were needed for the numerical solution to converge within 3% of the continuum solution.

Ramp Simulations

Simulation of ramp experiments were performed with a Monte Carlo algorithm. The long period ($>2 \times 10^{18}$) random number generator of L'Ecuyer with Bays-Durham shuffle (Press et al., 1992) was used to generate random numbers r_n with values between 0 and 1. Waiting times τ_{ab} of transitions from state a to state b were calculated from transformation of r_n. Unlike the situation where the membrane potential is held constant over the time course of simulation, the distribution of waiting times for an applied voltage ramp is not exponential since the value of the unidirectional rate constant α_{ab} changes with time. According to the theory of failure rate analysis (Papoulis, 1991), the probability density function $f(\tau_{ab})$ of the waiting time is:

$$f(\tau_{ab}) = \alpha_{ab}(\tau_{ab}) \exp\{-\int_0^{\tau_{ab}} \alpha_{ab}(t)\, dt\} . \quad (13)$$

We used an Arrhenius expression for the rate constant: $\alpha_{ab}(t) = \alpha^o_{ab} \exp\{q_{ab}x_{ab}V(t)/kT\}$. $V(t)$ is given by $V_o + mt$, where V_o is the ramp potential at time zero (i.e., the time at which the channel entered state a) and m is the ramp speed in units of voltage per unit time. The variable q_{ab} is the transition gating charge movement, and x_{ab} is the fractional position of the activation barrier between states a and b. By integrating the expression for conservation of probability, $f(\tau_{ab})d\tau_{ab} = f(r_n)dr_n$ (Papoulis, 1991), we obtain the following relationship between the random variables τ_{ab} and r_n:

$$\tau_{ab} = \frac{kT}{q_{ab}x_{ab}m} \ln \left[1 - \frac{q_{ab}x_{ab}m}{kT a^O_{ab}} \ln(1 - r_n) \exp\{-\frac{q_{ab}x_{ab}V_O}{kT}\} \right]. \quad (14)$$

In the event of competing transitions out of state a (multiple b states possible), selection was made by generating a waiting time for each one and choosing the smallest value. The single channel gating current record $i_g(t)$ was constructed by binning transition impulses weighted by q_{ab} onto the discretized time axis. For the single channel ionic current record $i(t)$, we used the formula $i = g(V - V_x)$, where g is the conductance of the resident state, and V_x is the reversal potential of the permeant ion(s). The single channel traces were digitally filtered using a Gaussian filter with cutoff frequency f_c and delay $1/2f_c$ (which approximates a multipole Bessel filter; see Crouzy and Sigworth, 1993) and accumulated to produce macroscopic currents. To obtain a quantity proportional to the open probability, the mean ionic current was divided by the driving force, $(V + 100)$ mV, for all ramp voltages V. Eq. 3 was used to obtain the sample estimate of the mean activation charge displacement, $\bar{q}_a$, except that the expression $\{dP_o/dV\}/P_o$ was evaluated instead of the equivalent $d(\ln P_o)/dV$ in order to reduce round-off error. The ramp Q-V curve was obtained from the integral of the mean gating current. The software used in numerical calculations and the Monte Carlo simulation was written in the C programming language and was run on a 60 mHz Pentium processor.

RESULTS

We now demonstrate the theory with a series of numerical examples illustrated by Figs. 2 through 8. Starting with the simple discrete state models (Figs. 2 through 4), one or more schematic state diagrams are shown in increasing value of q on the left side of each figure. Following standard kinetic notation, allowable transitions between discrete states are indicated by a line labeled with the corresponding gating charge movement. This is done mainly because a kinetic model is more familiar looking than a random assortment of disconnected states, but it must be kept in mind that the nature and arrangement of connections between states are irrelevant for calculations of equilibrium quantities (such as P_o and $\langle q_a \rangle$), so long as a path exists which connects all states, and the time required for equilibration is much shorter than the length of the experiment. It is easy to see that the theoretical equations derived earlier are in accordance with this general rule, and they hold for models with continuous as well as discrete densities of states.

For all models we considered, whether discrete or continuous, we set the total essential charge movement Δq_e equal to 4 eu to facilitate comparisons between models. Associated with each example are numerically derived plots of the equilibrium values of the gating charge displacement Q (normalized to one, as is normally done in practice) and the mean open probability P_o (actual value). The mean activation charge displacement $\langle q_a \rangle$ and the value of Δq-$\langle q \rangle$, also numerically derived, are featured in Fig. 2 *C*. Recall that the quantities

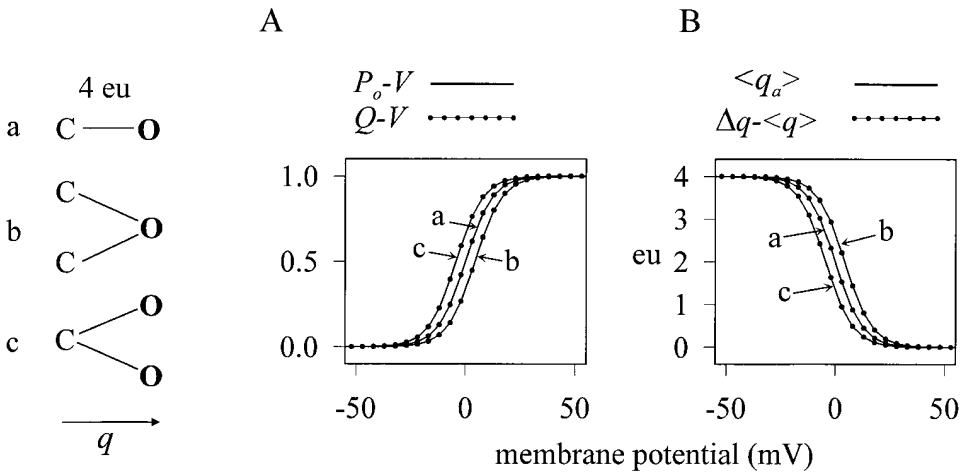

FIGURE 2. (*A*) Plots of open probability (P_o) and normalized gating charge displacement (Q) vs. voltage for a two-state model *a* and two models with degenerate states (*b* and *c*). (*B*) In each case, the mean activation charge displacement, $\langle q_a \rangle$, and the mean gating charge displacement, $\langle q \rangle$ (inverted and displaced by Δq), lie on the same plot, indicating that the channels are saturated.

Q and $\langle q \rangle$ are related by a factor of N, so they both have the same shape when normalized. Although we sometimes appear to use them interchangeably, we use Q when referring to experimental gating charge measurements where N is not known, whereas $\langle q \rangle$ is the mean of the single channel gating charge displacement, which is not directly measurable.

The discrete state models in Figs. 2 through 4 share the following features: the zero voltage potential G_i is the same for each state, though this is not explicitly shown in the figures. This tends to center the activation curves around $V = 0$. The closed states ($f = 0$) are labeled "C." Similarly, "O" stands for open ($f = 1$).

Two-state Model

Model 2*a* (Fig. 2) is a simple two state model, in which the total charge movement of 4 eu occurs in a single transition. A property of any two-state model is that all equilibrium properties lie on the same Boltzmann curve after normalization (Lumry et al., 1966). Thus the P_o-V and Q-V curves superimpose, and, because the two states are equipotential, the plots are centered around $V = 0$. Since there is only one open state and no peripheral charge movement, the model represents a saturated channel (see *Theory*). It is also the simplest example which satisfies Almers' criterion. Fig. 2 *B* shows the superposition of the plots of $\langle q_a \rangle$ and Δq-$\langle q \rangle$, which demonstrates graphically that the limiting value of $\langle q_a \rangle$ is reached only at potentials where the Q-V curve is close to saturating.

Three-state Nonsequential Models

We relax the restriction to linear sequential models with models *b* and *c* of Fig. 2. In both cases we see a parallel movement of 4 eu that either converges to a single open state (model 2*b*) or diverges into two open states (model 2*c*). The total range of gating charge movement for each model is not 8 eu, but rather 4 eu, since state probability is split equally among the two pathways. As a rule, the maximal charge movement of a model containing communicating parallel paths is simply the largest net charge movement of any of the possible pathways. Both models 2*b* and 2*c* represent saturated channels. In the case of model 2*c*, although there are two open states, they are degenerate with respect to q (ϕ(open) = 2), producing no latent charge movement. The addition of an extra state merely shifts each Boltzmann plot to one side, without a change in the steepness of the curve at midpoint. This is because a state degeneracy produces an increase in entropy in the respective state. For example, in model 2*b*, setting $V = 0$ distributes 2/3 of the system probability to the two closed states, which lowers $\langle q \rangle$ and P_o. The same reasoning applied to other potentials explains why the equilibrium curves for model 2*b* are shifted to the right on the voltage axis. Similarly, the degenerate open state of model 2*c* produces a shift to the left.

As mentioned earlier, a different arrangement of allowable transitions in a particular model does not change the equilibrium values of state variables. For example, in model 2*c*, a line could be drawn between the two open states, and one of the existing lines from the closed state deleted, and the results shown in Fig. 2, *A* and *B*, would be unchanged. However, the kinetics of activation, which are not of concern here, but are an important determinant of channel function, would be drastically altered by such a change.

Three-state Linear Sequential Models

In channels with three or more nondegenerate states, we do not expect activation curves representing different thermodynamic quantities to coincide. By inserting an extra closed state into the activation pathway of model 2*a*, we displace the P_o-V to the right of center and slightly broaden the Q-V (Fig. 3 *A*). However, this model remains saturated since it satisfies Almers' crite-

rion of a linear sequence of closed states followed by one open state. Thus, $\langle q_a \rangle$ and Δq-$\langle q \rangle$ superimpose (Fig. 3 *B*), and the limiting slope procedure could be accurately used to measure total charge movement per channel.

Switching the positions of the open state and its neighboring closed state results in model 3*b*, which now has a closed state at the end of the activation pathway. The *Q-V* curve is unchanged but the P_o-*V* now approaches zero at positive as well as negative potentials. An example of this behavior may be seen in a channel experiencing voltage-dependent block (Bezanilla and Armstrong, 1972). Here we have the first example in which the open state appears in the middle of the activation sequence, and so we expect $\langle q_l \rangle$ to have a finite (but constant) value. Indeed, we see that the plot of $\langle q_a \rangle$ vs. *V* is displaced downward by a constant value of 2 eu (Fig. 3 *D*). Consequently, $\langle q_a \rangle$ becomes negative at depolarizing potentials, which comes about because the open probability decreases with increasing positive potential. Note that the total range of $\langle q_a \rangle$, which we will refer to as $\Delta\langle q_a \rangle$, is still 4 eu, though the limiting slope value in the hyperpolarizing direction (which we will refer to as Δq_{a+}, see Figs. 1 *B* and 3 *D*) is only 2 eu and would by itself give an underestimate of Δq. Thus, in order to correctly estimate the entire range of gating charge movement in this case, one would also need to apply the limiting slope procedure to depolarized potentials to obtain the negative component of the mean activation charge displacement (Δq_{a-}). Model 3*b* remains an example of a saturated channel, since there is only one open state and no peripheral charge movement.

In the last model of Fig. 3 (model 3*c*), there are two open states in sequence at the end of activation. The *Q-V* curve is still unchanged, but now the P_o-*V* is shifted to the left of center. This is due to gating charge movement between open states, leading to a positive value for $\langle q_l \rangle$, which is now a function of voltage. This channel is not saturated. The range in mean activation charge displacement $\Delta\langle q_a \rangle$ reflects only the initial tran-

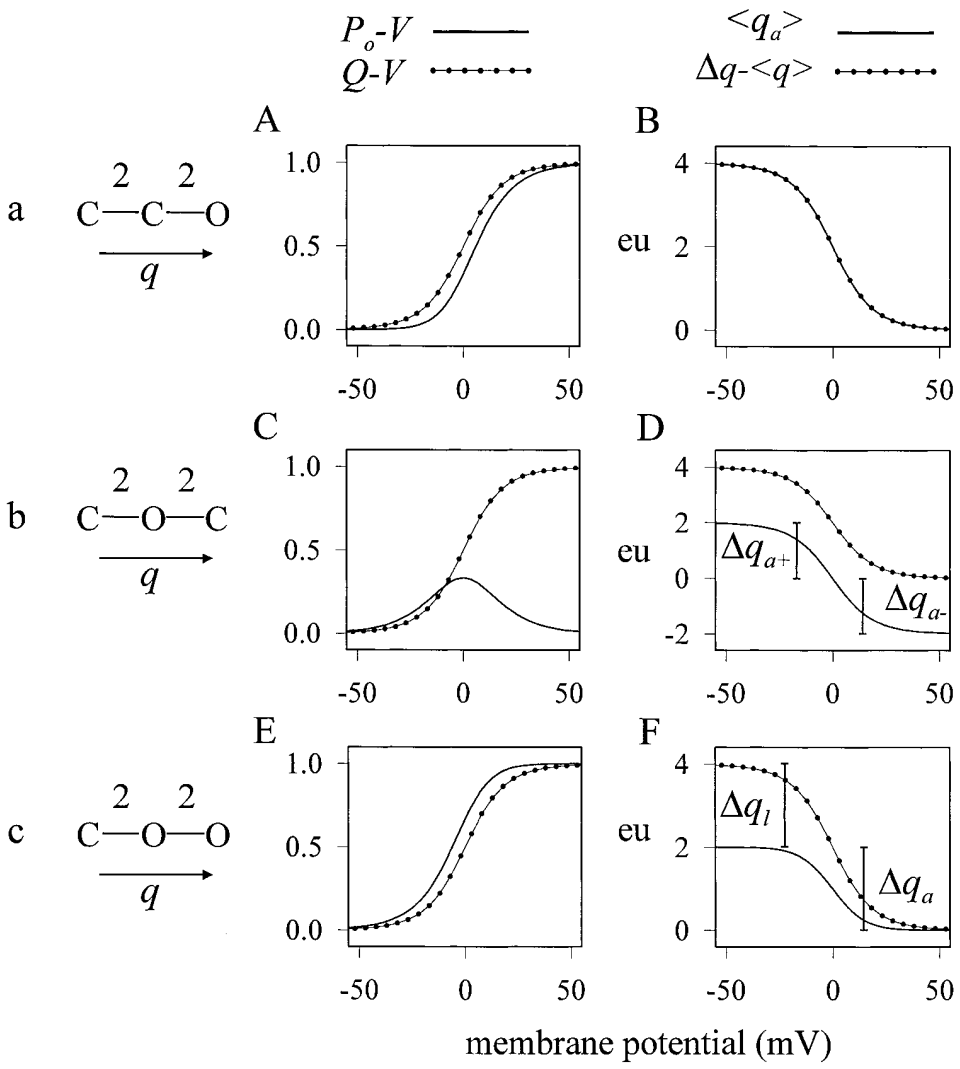

FIGURE 3. Model *a* is a linear three state scheme satisfying Almers' criterion. The P_o is displaced to the right of center (*A*), though the channel is saturated (*B*). The open probability in model *b* vanishes at both ends of the voltage axis (*C*). Consequently, it has a nonvanishing value for the latent charge displacement, splitting the activation charge displacement into positive and negative components (*D*). Model *c* has two open states, displacing $P_o(V)$ to the left of the *Q-V* (*E*), and resulting in a limiting slope estimate of only 50% of the total gating charge movement (*F*).

sition from the closed to the first open state. Hence the limiting slope procedure applied to this particular model underestimates Δq by one half its value. In contrast, the Q/N procedure will give the correct value of Δq for this model since it measures all essential charge movement. Although model 3*c* is displayed in Fig. 3 as a linear sequential model, the same outcome arises from a branching model in which a closed state makes transitions to two open states with respective gating charge movements, 2 eu and 4 eu (compare to model 2*c*, but with unequal charge movement per leg). Branching models, although useful in studying kinetics, are no different than linear sequential models in their equilibrium properties.

Models with Peripheral Charge

In Fig. 4 we demonstrate the effects of charge movement energetically uncoupled to the main activation pathway (peripheral charge movement). Model 4*a* represents a saturated channel with a looped network of four closed states converging to an open state. The range in gating charge displacement Δq is 4 eu and is entirely essential. By severing the links between the upper and lower charge relay systems, we obtain model 4*b*, which has two independent charge systems, with only the lower one linked to activation. If one were to measure the total range of $\langle q \rangle$ in this fragmented model, one would find it to be 6 eu, not 4 (if this is not immediately obvious, consider that we routinely sum the charge movements of N independent channels to obtain the gating current; also, the sum of all state probabilities in model 4*b* gives two, rather than one as in model 4*a*). The range in essential charge movement is unchanged (Δq_e = 4 eu), but now, due to the additional peripheral charge movement Δq_p of 2 eu, there is a mismatch between the limiting value of $\langle q_a \rangle$, which correctly estimates Δq_e, and that of $\Delta q = \Delta q_{Q/N}$, the value obtained if one were using the Q/N procedure. An example of peripheral charge movement present in neuronal α_{1E} Ca^{2+} channels has recently been demonstrated (Noceti et al., 1996) — in absence of the β_{2a} regulatory subunit, there appears to be a parallel charge system that, on the time scale of the observations, is kinetically isolated from the main activation sequence of the channel, leading to a $\Delta q_{Q/N}$ value of 14 eu, but a value of only 9 eu for Δq_e. With addition of the β_{2a} subunit to the system, the Q/N value dropped to the value of the limiting slope, which remained at 9 eu, suggesting that there was a lowering of the energy barrier which had separated the 5 eu of peripheral charge movement from the remainder, resulting in faster equilibration between the two charge systems. The β_{2a} subunit has no significant effect (<10 mV) on the half activation potential of the mean gating charge displacement or the initial rise of the open probability (Olcese et al., 1996), meaning that it is unlikely that the limiting slope value before addition of subunit was being selectively underestimated due to a larger voltage separation between the Q-V and the P_o-V plots.

Models with Continuous Distribution of States

In Figs. 5 through 7, we shift our focus to continuous systems, where we will confirm some of the observa-

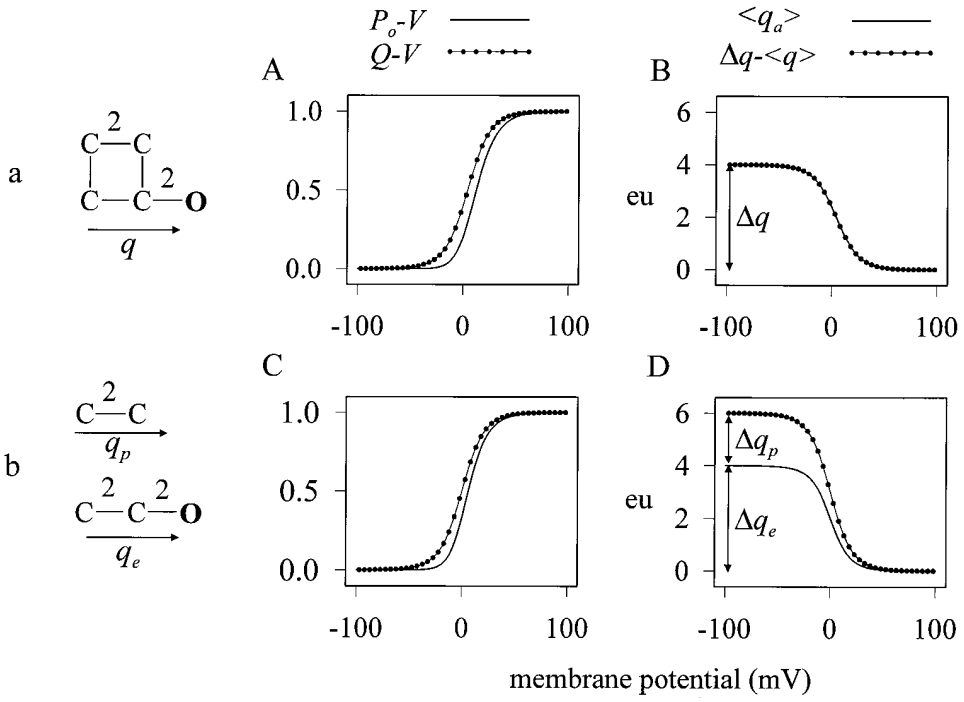

FIGURE 4. (*A* and *B*) Model *a* represents a saturated channel with a closed loop of nonconducting states followed by one open state; Δq = 4 eu. By severing the connections indicated by the vertical lines (model *b*), we obtain two independent charge relay systems: one essential, moving 4 eu of gating charge (Δq_e), and the other peripheral, moving 2 eu (Δq_p). In addition to a slight shift to the right of the P_o-V (*C*), the channel becomes unsaturated (*D*), though use of the limiting slope procedure in this case would produce the correct estimate of essential gating charge movement ($\Delta q_a = \Delta q_e$).

tions made above with discrete state systems, and encounter some new behavior. In these figures, the left side shows the potential profile $G(q)$ as well as the fractional conductance $f(q)$.

We begin with a flat free energy landscape for Fig. 5, which is implicitly the same assumption we have been making for all of the discrete state models described so far. The charge density is confined to within the boundaries $q = 0$ and $q = \Delta q = 4$ eu. The function $f(q)$ is zero (corresponding to closed states) for lower values of q, and then undergoes an abrupt change at $q = a\Delta q$ to a value of one (open state), where it remains until it reaches the upper boundary of q. Thus, this model has a varying amount of saturation which increases with the value of a. Of the discrete models we have considered so far, the most analogous to this model would be the model 3*c* of Fig. 3, since both are linear sequential (no degeneracies) with a finite amount of charge movement between open states. We concluded earlier in the discussion of Fig. 3 that the limiting value of $\langle q_a \rangle$ could never reach Δq due to latent charge movement. This is shown to be the case as well with the continuum model, where it is apparent from Fig. 5 *B* that $\langle q_a \rangle$ reaches the maximum value of $a\Delta q$. Note also the crossing of P_o-V with the normalized Q-V in Fig. 5 *A*, indicating the presence of multiple open states.

In Fig. 6 we demonstrate the effect of broadening $f(q)$ around the gating charge position $q = 0.9\Delta q$. We notice immediately a striking difference between the plots of $\langle q_a \rangle$ in Fig. 6 and those we have seen so far. The value of $\langle q_a \rangle$ plateaus without reaching the maximum value Δq, and then appears to shrink to zero with increasing negative potential. The effect is more pronounced for broad distributions of $f(q)$ than for very sharp ones. It would be quite interesting to see experimental evidence of the fall-off of $\langle q_a \rangle$ at negative potentials, since it would support the notion of subconductance states along the activation pathway. Incidently, a similar effect occurs in a discrete model similar to model 3*c*, if the last transition (between open states) moves significantly more charge than the first, leading to an early plateau in $\langle q_a \rangle$, which can be significantly larger in magnitude than the eventual limiting value seen at hyperpolarized potentials.

We choose for our final continuum model (Fig. 7) one which approximates a two-state model. Instead of a flat potential profile, we now introduce an inverted parabolic peak 4 kT high with a slight flattening at the edges and bounded on the q-axis at $q = 0$ and $q = \Delta q = 4$. The channel is fully open for q values greater then $0.9 \cdot \Delta q$. The result is a slightly broader equilibrium curve than for the true two state model (Fig. 2), and the P_o-V curve is a bit shifted to the right of the Q-V. However, the $\langle q_a \rangle$ and Δq-$\langle q \rangle$ plots coincide enough to make the difference in their limiting values (as could be obtained from limiting slope and Q/N methods, respectively) difficult to resolve experimentally, if this were a real channel.

Multi-state Model with Subconductance States

Our concluding model (Fig. 8) shows that bizarre behavior of the equilibrium curves is not limited to continuum models. This model is discrete with five states. In contrast to the earlier discrete models we considered, we assign a different potential to each state, and we add subconductance states. Due to the small number of states, the plots of P_o and Q follow a somewhat erratic pathway. In a continuum model with a similar free energy landscape and the same approximate increase in $f(q)$, the P_o vs. V and Q-V would broaden out and appear smoother. The voltage dependence of $\langle q_a \rangle$ shows some interesting behavior, increasing from zero at positive potentials to a local peak of about $1/4\ \Delta q$, then dipping nearly to zero at more negative potentials, only to rise again to a maximum value slightly higher than that of the initial peak. Clearly, a plateau in the value of $\langle q_a \rangle$ may be misleading since it does not always represent the limiting slope value. The only way to be sure one has reached the final plateau is through

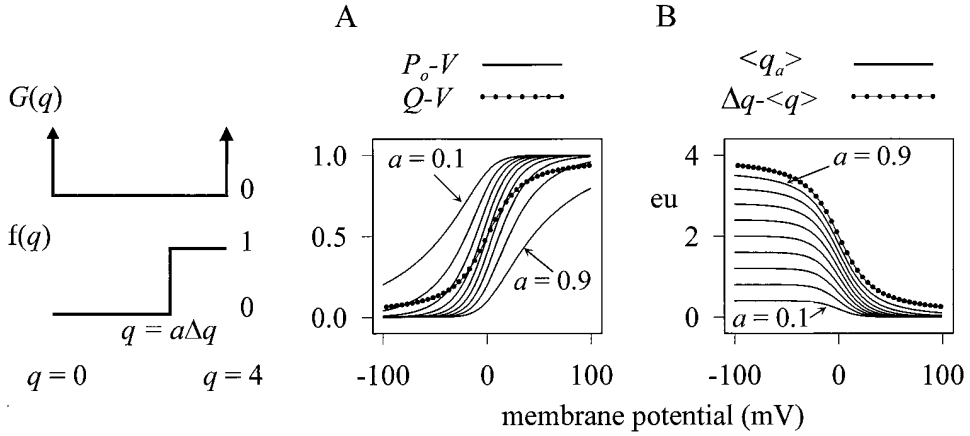

FIGURE 5. Predictions from a continuum model with a flat potential landscape. The transition from closed to open pore is abrupt and occurs at the value $a\Delta q$, where a ranges from 0.1 to 0.9 in increments of one-tenth. (*A*) As the value of a decreases, the P_o-V curve crosses the Q-V at increasingly negative potentials. (*B*) The limiting value of $\langle q_a \rangle$ is equal to range of gating charge movement that occurs when the channel is closed.

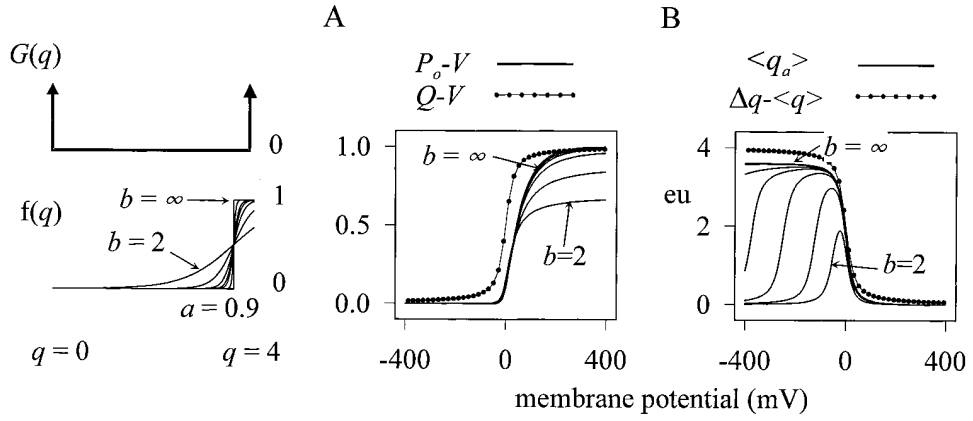

FIGURE 6. A continuum model with a slower rise of the fractional conduction along the q axis. The equation used for $f(q)$ is $[1 + \exp(-b(q - a\Delta q)]^{-1}$ where the slope factor b takes on the values: 2, 5, 10, 15, 20, 50, and infinity. The case of b = infinity is identical to the model in Fig. 5 with a = 0.9. A shallow slope lowers the open probability at extreme depolarizing potentials (*A*) and produces a downward shift in the mean activation charge displacement at hyperpolarized potentials (*B*).

comparison with the *Q-V*, which must be saturated in the range of potentials from which the limiting slope is recorded.

DISCUSSION

With the recent advances in molecular biology it has become possible to neutralize amino acids that are suspected to be voltage-sensing residues in ion channels and study the effects on gating. An important measure of channel responsiveness to voltage is the total charge movement of activation Δq. A significant reduction of Δq has been found after removal of charged residues in the S2 and S4 transmembrane domains of the *Shaker* potassium channel, indicating that these residues play an active role as components of the gating apparatus of the channel (Aggarwal and MacKinnon, 1996; Seoh et al., 1996). Almers (1978) summarized two methods by which one can obtain Δq: (*a*) the *Q/N* procedure, which requires that one measure the maximum range of gating charge movement and the number of channels in the same preparation, and (*b*) the limiting value of the logarithmic potential sensitivity (similar to our mean activation charge displacement $\langle q_a \rangle$, except that $P_o/[1 - P_o]$ replaces P_o as the argument of the logarithmic function), which equals the essential component of Δq in the absence of latent charge movement.

Using a statistical mechanics approach, we have expanded on Almers' theory by explicitly expressing $\langle q_a \rangle = kT\mathrm{d}(\ln P_o)/\mathrm{d}V$ as a function of gating charge displacement, and by generalizing the result to include parallel activation pathways, multiple open states, subconductance states, and continuum models. The outcome of the derivation can be summarized by the following relation:

$$kT\frac{\mathrm{d}\ln P_o}{\mathrm{d}V} + \langle q_l \rangle = \Delta q - \langle q \rangle . \qquad (15)$$

In cases where the ion channel is saturated and $\langle q_l \rangle$ is zero, Eq. 15 reduces to Almers' original expression for the limiting slope (Eq. 1) at hyperpolarizing potentials where the *Q-V* curve saturates ($\langle q \rangle = 0$).

A major obstacle in correctly estimating Δq using the limiting slope method is the accurate determination of $\langle q_a \rangle$ at potentials where the open probability is vanishingly small. This problem has been discussed by several authors (Andersen and Koeppe, 1992; Bezanilla and Stefani, 1994; Zagotta et al., 1994), but no criterion has

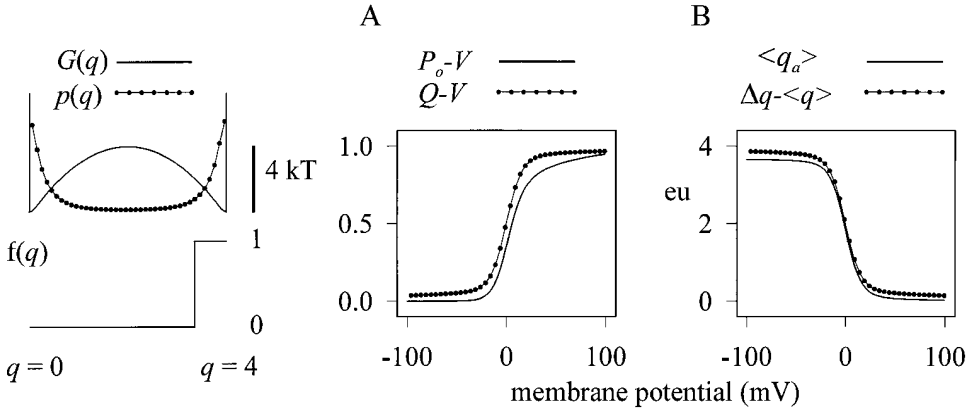

FIGURE 7. A continuum model that approximates a two-state discrete model. The probability density $p(q)$ for zero voltage is calculated from the potential of mean force $G(q)$ using the Boltzmann distribution. The channel opens when the gating charge displacement reaches $0.9 \cdot \Delta q$. Panels *A* and *B* are comparable to those of Fig. 2, model 2*a*.

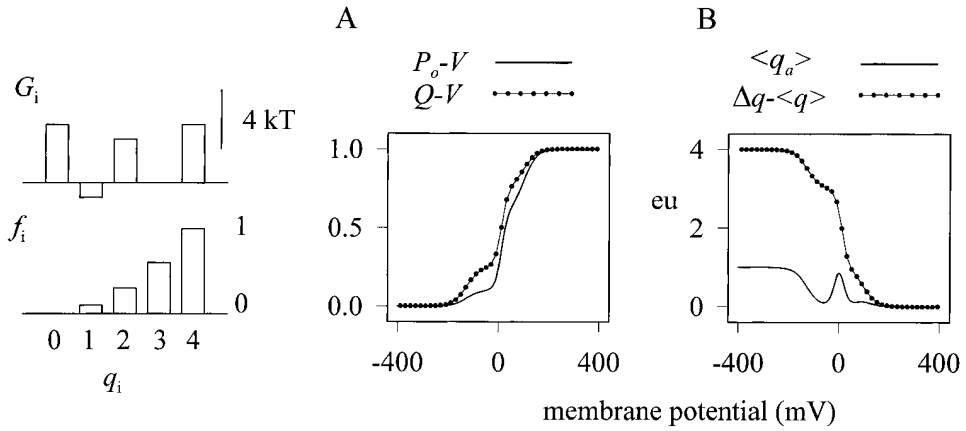

FIGURE 8. A 5-state model with subconductance states and varying potential landscape. The values of G and f in increasing order of q are $G_i = \{4, -1, 3, 0, 4\}kT$ and $f_i = \{0, 0.1, 0.3, 0.6, 1.0\}$. (*B*) The initial rise in $\langle q_a \rangle$ at $V \simeq 0$ mV could be mistaken for the value of the limiting slope under conditions of poor experimental resolution, but knowledge of the *Q-V* would indicate that the gating charge had not yet saturated.

been given to accept or reject the estimate except to take the value as a lower limit of the actual Δq. A useful guideline is provided by plotting $\langle q_a \rangle$ as a function of V or P_o (Zagotta et al., 1994) where it is possible to visualize whether the estimate shows signs of reaching a limiting value. Such limiting values have been observed in a few cases through single channel analysis in sodium channels (Hirschberg et al., 1996) or with macroscopic currents in neutralization mutants of *Shaker* K^+ channels (Noceti et al. 1996; Seoh et al., 1996). Often, however, poor experimental resolution prohibits the measurement of a sufficiently low value of P_o, making a prediction of where the value of $\langle q_a \rangle$ saturates extremely useful. This is possible, based on Eq. (16), if the *Q-V* curve is known and the channel is saturated. What needs to be done is to invert the *Q-V* curve and scale it so that it superimposes onto the incomplete plot of $\langle q_a \rangle$ vs. *V*. It is important that a large enough range of voltage is used to insure good overlap between the two curves so that proper scaling is achieved. The value of Δq is then read off from the scaled *Q-V* curve (Seoh et al., 1996).

An example of estimating Δq with limited resolution data is shown in Fig. 9. The data was obtained from a Monte Carlo simulation of gating and ionic currents following a ramp voltage protocol (see METHODS). The model is shown in the lower right corner of Fig. 9 and has five closed states followed by an open state. All five transitions move an identical amount of gating charge for a total of $\Delta q = 10$ eu. The ramp protocol is a useful experimental tool since it allows measurements of the signal for a large number of voltages in a single record. This is important when one is required to differentiate a measured quantity with respect to voltage, as we do when evaluating Eq. 3. The drawback in the method is that the ramp speed must be infinitely slow (quasistatic) for the channel to remain close to equilibrium during the ramp. Nevertheless, the alternative procedure of obtaining equilibrium values of ionic and gating currents from an activation series of pulses can be prohibitively difficult if one desires very fine resolution in voltage, making the ramp protocol the method of choice in certain cases (e.g., the presence of rundown in the preparation). In our simulation the midpoint of the integral of the mean gating current was shifted +2.5 mV with respect to the midpoint of the numerically derived *Q-V*, indicating that the quasistatic condition was not rigorously adhered to. This error will be evident in the final result. Fig. 9 *B* contains three plots. The estimate $\bar{q}_a$ and the ramp *Q-V* were calculated from the averaged ionic and gating currents plotted in Fig. 9 *A*. The numerical *Q-V* was derived from the model (experimentally, it can be accurately obtained from a voltage series of long pulses, Stefani et al., 1994). It is apparent that the scatter in $\bar{q}_a$ increases significantly with low P_o due to the increasing rarity of open events. The minimum value of P_o obtained in the plot of $\bar{q}_a$ was 5×10^{-3}, which is insufficient to reach the expected limiting value of 10 eu. Because the model satisfies Almers' criterion, we can use the inverted *Q-V* curves to "predict" the value of Δq by scaling them so they superimpose onto the foot of the plot of $\bar{q}_a$ vs. *V*. We see that, due to the insufficiently slow ramp speed, the predictions from the ramp *Q-V* curve and true *Q-V* curve are both 10% in error, with the real value of Δq lying approximately in between the two values. Thus, experimentally, it is important to use as slow a ramp speed as possible. This procedure was applied to the *Shaker* B K^+ channel and charge neutralization mutants by Seoh et al. (1996). Their results show that for many of the mutations on the S2 and S4 putative transmembrane domains, the inverted and scaled *Q-V* curve superimposes on the $\bar{q}_a$ vs *V* curve. The predicted value of the limiting slope matched the value of Δq obtained by the Q/N procedure, providing an internal check for consistency and at the same time showing that all charge that moves in *Shaker* is energetically coupled to the open state.

We conclude our discussion by suggesting an approach for measuring total gating charge movement in a generalized ion channel. A useful analysis should separate the gating charge into its components of periph-

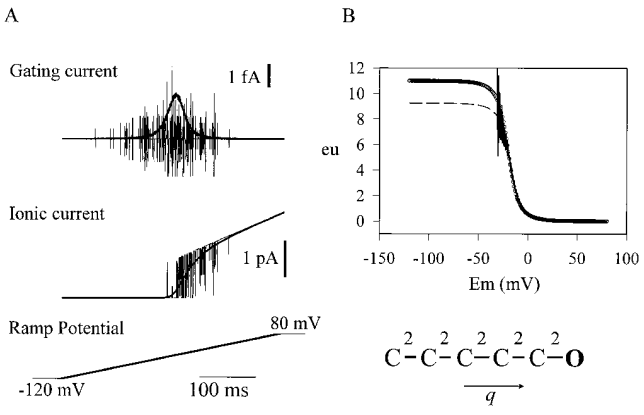

FIGURE 9. (*A*) Representative single channel traces (*thin line*) of simulated gating (*top*) and ionic (*middle*) currents using a voltage ramp protocol (*bottom*). The model (shown at the lower right of the figure) is discrete and saturated; $\Delta q = 10$ eu. The forward and backward rates at zero potential for all transitions were 5 and 1 ms^{-1}, respectively. The transition charge movements were 2 eu. Symmetric barriers were used. The times of transition events were obtained using Eq. 14. Single channel traces were then constructed and discretized at 101.3 μs with 4,000 points, and subsequently filtered (cutoff frequency 1 kHz) using a digital Gaussian filter with 0.5-ms delay. The mean of 10^6 accumulated single channel gating and ionic currents (*thick line*) are superimposed onto a corresponding representative single channel trace (*noisy thin line*). The mean gating current was scaled up by a factor of 50 to make it comparable to the single channel trace. (*B*) The sample estimate of the mean activation charge displacement $\bar{q}_a$ (*solid line*) and the *Q-V* curve (*dashed line*) were derived from the ramp data (see METHODS). The true *Q-V* (*unfilled circles*) was calculated numerically every 1 mV using the formula for $\langle q \rangle$ given in the theory section. Both *Q-V* curves were inverted and independently rescaled to superimpose on the smooth region of $\bar{q}_a$.

eral, latent, and activation charge displacements. Latent charge movement comes about when gating charge moves during a transition between two or more discrete open or subconductance states, or along a continuum. Analysis of single channel records may uncover kinetically distinct discrete open states and/or subconductance states. Rate constants between successive open states may be voltage dependent, suggesting latent charge movement. Another useful test for the presence of latent charge movement in a channel that opens with depolarization is performed by comparing P_o-*V* and *Q-V* traces gathered from macroscopic currents. If the two plots cross, or if the P_o is shifted to the left of the *Q-V*, latent charge movement exists and the limiting slope procedure will underestimate the range of essential charge movement (e.g., Fig. 3 *F*). Oftentimes, noise analysis of macroscopic ionic currents is easier to carry out than single channel analysis. In such cases, a nonparabolic variance vs. mean plot of nonstationary ionic currents (Steffan and Heinemann, 1996) points at the presence of subconductance states. Also, autocovariance analysis of stationary macroscopic ionic currents can detect multiple open states (Sigworth, 1981). If the channel has latent charge movement, it is not saturated with activation charge, and the range of activation charge Δq_a is necessarily less than the range of essential charge movement Δq_e. It must be kept in mind that the complete range in $\langle q_a \rangle$ spans from maximally negative to maximally positive potentials, and in cases where the channel closes with extreme potential on either side of the voltage axis, the limiting slope procedure must be carried out at positive as well as negative potentials (e.g., Fig. 3 *D*). In a saturated channel, the limiting slope procedure can be used to estimate Δq_e, but lack of experimental resolution often makes it difficult to determine at which potential a limiting value of the activation charge displacement is reached. This is where the *Q-V* plot becomes invaluable, since the *Q-V* and the $\langle q_a \rangle$-*V* plots plateau at the same voltage range in saturated channels. The value of *Q* is easier to measure than $\langle q_a \rangle$ (assuming ionic currents can be effectively eliminated) near the region of limiting slope, since the relation of *Q* with gating charge displacement is linear, whereas that of $\langle q_a \rangle$ to P_o is obtained through differentiation, which amplifies the measurement error. Thus, the *Q-V* is a much more sensitive tool at determining the voltage at which $\langle q_a \rangle$ will saturate and can even be used to predict the value of Δq_e from low-resolution data (Fig. 9). There may be instances when a *Q-V* is unobtainable (inadequate expression of channels, incomplete blocking of the pore, etc.). In such cases, an alternate method (Cole-Moore shift) for determining whether $\langle q_a \rangle$ has reached its final value may prove useful as a last resort. The Cole-Moore shift is defined as the time delay of opening of the channel as a function of holding potential (Cole and Moore, 1960; Stefani et al., 1994)). At those potentials where $\langle q_a \rangle$ has reached saturation, the delay should also have reached its maximum value. It should be kept in mind, however, that the Cole-Moore shift is a kinetic measurement, even though its voltage dependence arises from the equilibrium probability distribution at the holding potential. Thus, unlike the *Q-V*, the plot of opening delay vs. voltage has no functional relationship with $\langle q_a \rangle$ vs. voltage. Nevertheless, the initial probability distribution does not change beyond the voltage at which the gating charge saturates, so in principle the Cole-Moore shift, if accurately measured, could serve as a poor man's *Q-V* in limiting slope experiments.

A separate issue is whether or not there is contamination of the gating charge movement with a peripheral (independent) charge system. Peripheral charge movement shows up in the *Q/N* estimate of total gating charge movement, so $\Delta q_{Q/N}$ will be larger than Δq_e in the presence of peripheral charge. Combining this result and the earlier one, which set the upper limit of Δq_a as Δq_e, we obtain the inequality:

$$\Delta q_a \leq \Delta q_e \leq \Delta q_{Q/N}. \quad (16)$$

If the values of Δq_a and $\Delta q_{Q/N}$ are the same, it is a good indicator that there is neither latent nor peripheral charge movement, and the estimate of Δq_e is an accurate one. If both latent and peripheral charge are associated with the same channel, it may be difficult to determine the contribution of each. In such a case, kinetic modeling might be required in order to estimate the amount of charge movement between open states through the voltage dependence of the transition rate constants.

In summary, when measuring Δq_e, the range in essential charge movement in a single channel, it is desirable to obtain the full activation curves of the open probability and gating charge displacement. For channels without latent charge movement, the limiting slope procedure, in conjunction with information from the *Q-V* plot, will produce an accurate estimate of Δq_e. In the general case, the value of Δq_e will lie between the range of activation charge displacement, Δq_a, and the total charge movement per channel, $\Delta q_{Q/N}$, obtained from the limiting slope method and *Q/N* procedure, respectively.

We thank Drs. Dorine Starace, David E. Patton, Francesca Noceti, and Enrico Stefani for reading and commenting on the manuscript.

This work was supported by United States Public Health Service grant GM30376 and a Dissertation Fellowship from the Graduate Division at UCLA to D. Sigg.

Original version received 21 June 1996 and accepted version received 16 September 1996.

REFERENCES

Aggarwal, S.K., and R. MacKinnon. 1996. Contribution of the S4 segment to gating charge in the *Shaker* K^+ channel. *Neuron.* 16: 1169–1177.

Almers, W. 1978. Gating currents and charge movements in excitable membranes. *Rev. Physiol. Biochem. Pharmacol.* 82:96–190.

Andersen, O.S., and R.E. Koeppe II. 1992. Molecular determinants of channel function. *Physiol. Rev.* 72:S89–S158.

Armstrong, C.M., and F. Bezanilla. 1973. Currents related to movement of the gating particles of the sodium channels. *Nature (Lond.).* 242:459–461.

Bezanilla, F., and C.M. Armstrong. 1972. Negative conductance caused by entry of sodium and cesium ions into the potassium channels of squid axons. *J. Gen. Physiol.* 60:588–608.

Bezanilla, F., and E. Stefani. 1994. Voltage-dependent gating of ionic channels. *Annu. Rev. Biophys. Biomol. Struct.* 23:819–846.

Cole, K.S., and J.W. Moore. 1960. Potassium ion current in the squid giant axon: dynamic characteristics. *Biophys. J.* 1:1–14.

Crouzy, S.C., and F.J. Sigworth. 1993. Fluctuations in ion channel gating currents. Analysis of nonstationary shot noise. *Biophys. J.* 64:68–76.

Hirschberg, B., A. Rovner, M. Lieberman, and J. Patlak. 1996. Transfer of twelve charges is needed to open skeletal muscle Na^+ channels. *J. Gen. Physiol.* 106:1053–1068.

Hodgkin, A.L., and A.F. Huxley. 1952. A quantitative description of membrane current and its application to conduction and excitation in nerve. *J. Physiol. (Lond.).* 117:500–544.

Liman, E.R., F. Weaver, G. Koren, and P. Hess. 1991. Voltage-sensing residues in the S4 region of a mammalian K^+ channel. *Nature (Lond.).* 353:752–756.

Lumry, R., R. Biltonen, and J.F. Brandts. 1966. Validity of the "two-state" hypothesis for conformational transitions of proteins. *Biopolymers.* 4:917–944.

Noceti, F., P. Baldelli, X. Wei, N. Qin, L. Toro, L. Birnbaumer, and E. Stefani. 1996. Effective Gating charges per channel in voltage-dependent K^+ and Ca^{2+} Channels. *J. Gen. Physiol.* 108:143–156.

Olcese, R., A. Neely, N. Qin, X. Wei, L. Birnbaumer, and E. Stefani. 1996. Coupling between charge movement and pore opening in neuronal α_{1E} calcium channels. *J. Physiol. (Lond.).* In press.

Papazian, D.M., L.C. Timpe, Y.N. Jan, and L.Y. Jan. 1991. Alteration of voltage-dependence of *Shaker* potassium channel by mutations in the S4 sequence. *Nature (Lond.).* 349:305–310.

Papoulis, A. 1991. Probability, Random Variables, and Stochastic Processes. 3rd ed. McGraw-Hill. New York. 666 pp.

Press, W.H., S.A. Teukolsky, W.T. Vetterling, and B.P. Flannery. 1992. Numerical Recipes in C: The Art of Scientific Computing. 2nd ed. Cambridge University Press. Cambridge, UK. 994 pp.

Schoppa, N.E., K. McCormack, M.A. Tanouye, and F.J. Sigworth. 1992. The size of gating charge in wild-type and mutant *Shaker* potassium channels. *Science (Wash. DC).* 255:1712–1715.

Seoh, S.-A., D. Sigg, D.M. Papazian, and F. Bezanilla. 1996. Voltage-sensing residues in the S2 and S4 segments of the *Shaker* K^+ channel. *Neuron.* 16:1159–1167.

Sigworth, F.J. 1981. Covariance of nonstationary sodium current fluctuations at the node of ranvier. *Biophys. J.* 34:111–133.

Stefani, E., L. Toro, E. Perozo, and F. Bezanilla. 1994. Gating of shaker K^+ channels. 1. Ionic and gating currents. *Biophys. J.* 66:996–1010.

Steffan, R., and S.H. Heinemann. 1996. Resolution limits of nonstationary noise analysis determined with computer simulations. *Biophys. J.* 70:A396. (Abstr.).

Stimers, J.R., F. Bezanilla, and R.E. Taylor. 1985. Sodium channel activation in the squid giant axon. *J. Gen. Physiol.* 85:65–82.

Tsien, R.W., and D. Noble. 1969. A transition state theory approach to the kinetics of conductance changes in excitable membranes. *J. Memb. Biol.* 1:248–273.

Zagotta, W.N., T. Hoshi, J. Dittman, and R.W. Aldrich. 1994. *Shaker* potassium channel gating II. Transitions in the activation pathway. *J. Gen. Physiol.* 103:279–319.